

Nonlinear Static Analysis of Laminated Composite Hollow Beams with Super-Elliptic Cross-Sections

G. Akgun, I. Algul, H. Kurtaran

Abstract—In this paper geometrically nonlinear static behavior of laminated composite hollow super-elliptic beams is investigated using generalized differential quadrature method. Super-elliptic beam can have both oval and elliptic cross-sections by adjusting parameters in super-ellipse formulation (also known as Lamé curves). Equilibrium equations of super-elliptic beam are obtained using the virtual work principle. Geometric nonlinearity is taken into account using von-Kármán nonlinear strain-displacement relations. Spatial derivatives in strains are expressed with the generalized differential quadrature method. Transverse shear effect is considered through the first-order shear deformation theory. Static equilibrium equations are solved using Newton-Raphson method. Several composite super-elliptic beam problems are solved with the proposed method. Effects of layer orientations of composite material, boundary conditions, ovality and ellipticity on bending behavior are investigated.

Keywords—Generalized differential quadrature, geometric nonlinearity, laminated composite, super-elliptic cross-section.

I. INTRODUCTION

COMPOSITE beams with various cross-sectional shapes such as circular, rectangular or elliptic in solid or hollow form are used in many engineering fields like civil engineering, aeronautics, military, automotive and marine industry as reinforcement elements or load carrying structures. Hence, understanding the mechanical behavior of these structures is very essential to enable safe and economical designs. Following studies from literature are related to the beams with various cross-sectional shapes such as circular, rectangular or elliptic in solid or hollow form. Guo et al. [1] conducted an experimental study on the bending behavior of thin-walled circular hollow section tube structures. Karagiozova et al. [2], [3] studied on the dynamic response of circular and square metallic hollow cross-section beams subjected to an impulsive loading in order to investigate the deformation and energy absorption characteristics of such structures. Zheng et al. [4] investigated the bending capacity of cold-formed stainless steel beams with rectangular and circular cross-section both experimentally and numerically. Li and Yang [5] studied on thermal post-buckling behavior of anisotropic laminated beams with tubular cross-sections resting on elastic foundation under a variety of temperature distributions through the thickness. Asadi and Aghdam [6] performed large amplitude free vibration and post-buckling

analysis of laminated composite beam with non-uniform cross-section resting on a nonlinear elastic foundation using Euler–Bernoulli beam theory and GDQ method. Zhao et al. [7] used Chebyshev polynomials theory to investigate the free vibration behavior of functionally graded Euler–Bernoulli and Timoshenko beams with non-uniform cross-sections. Ghafari and Rezaeepazhand [8] employed dimensional reduction method in order to perform an isogeometric analysis on composite beams with arbitrary cross-section. Jiao et al. [9] conducted both theoretical and experimental studies on the buckling and post-buckling behavior of bilaterally constrained beams with non-uniform cross-sections. Law and Gardner [10] investigated the lateral instability of beams with elliptical hollow cross-section. Murin et al. [11] conducted experimental, numerical and semi-analytical studies on torsional warping free vibration behavior of rectangular hollow beams.

As it can be seen from the literature, there are studies about beams with various cross-sections. In this study circular, elliptical or oval cross-sections can be expressed through super-ellipse formulation. Thus, in this study, geometrically nonlinear static behavior of laminated composite hollow beams with super-elliptic cross sections is investigated using generalized differential quadrature (GDQ) method. Static equilibrium equations are obtained through virtual work principle and von-Kármán nonlinear strain-displacement relations are utilized to represent the geometric nonlinearity. Transverse shear effect is taken into account according to the first-order shear deformation theory. Newton-Raphson method is used to solve equilibrium equations. Several laminated composite super-elliptic beam problems are solved using GDQ method to investigate bending behavior under different boundary conditions considering different layer orientation angle, ovality and ellipticity values.

II. STATEMENT OF THE PROBLEM

Cross-section of a super-elliptical beam is formed with Lamé curves defined by

$$\left| \frac{y}{a} \right|^n + \left| \frac{z}{b} \right|^n = 1 \quad (1)$$

where a and b are the major and minor radius at a cross-section. a/b ratio defines the ellipticity of the cross-section. n is a positive number determining the ovality of the cross-section. The curve is called as ellipse for $n = 2$, hypo-ellipse for $n < 2$ and hyper-ellipse for $n > 2$. The ovality of the cross-

G. A. and I. A. are with the Department of Mechanical Engineering, Gebze Technical University, Gebze – Kocaeli, Turkey (phone: +90 262 605 27 88; e-mail: agokce@gtu.edu.tr, ilkees@gtu.edu.tr).

H. K. is with the Department of Mechanical Engineering, Gebze Technical University, Gebze – Kocaeli, Turkey (phone: +90 262 605 27 78; e-mail: hasan@gtu.edu.tr).

section increases with increasing value of n as it is shown in Fig. 1. Dimensional properties of super-elliptic beam are shown in Fig. 2 where t is the wall thickness, h and L are the height and length of the beam, respectively.

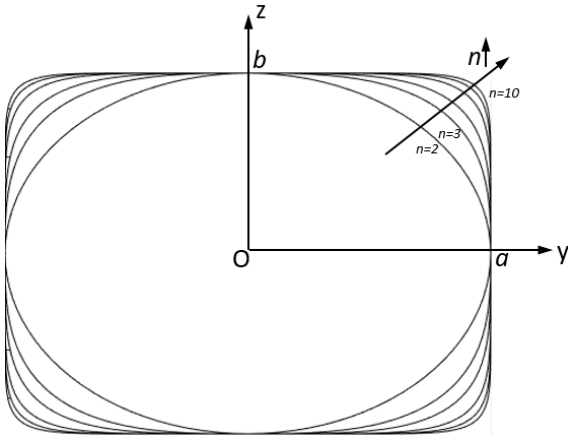


Fig. 1 Cross section of a beam with different Lamé curves

In a moderately thick beam, based on first-order shear deformation theory (FSDT) displacement field can be written in terms of mid-plane displacements and rotation as

$$\begin{aligned} u(x, z) &= u_0(x) + z\theta_x(x) \\ w(x, z) &= w_0(x) \end{aligned} \quad (2)$$

where u_0 , w_0 denote longitudinal and transverse displacements at reference mid-plane (x - y) and θ_x represents the rotation about y axis.

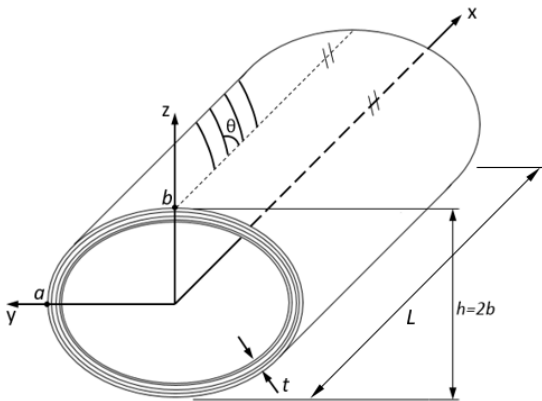


Fig. 2 Hollow cross section parameters and fiber orientation for laminated composite

Nonlinear strain components for moderately thick beam can be expressed as [12]

$$\begin{aligned} \varepsilon_x &= \varepsilon_0 + z \cdot \varepsilon_1 \\ \gamma_{zx} &= \varepsilon_s \end{aligned} \quad (3)$$

where

$$\begin{aligned} \varepsilon_0 &= \frac{\partial u_0}{\partial x} + \frac{1}{2} \cdot \left(\frac{\partial w_0}{\partial x} \right)^2 \\ \varepsilon_1 &= \frac{\partial \theta_x}{\partial x} \\ \varepsilon_s &= \theta_x + \frac{\partial w_0}{\partial x} \end{aligned} \quad (4)$$

The constitutive equation for a laminated composite beam can be expressed in terms of in-plane force and moment resultants as

$$N = \begin{Bmatrix} N_1 \\ N_2 \end{Bmatrix} = \begin{bmatrix} A & B \\ B & D \end{bmatrix} \cdot \begin{Bmatrix} \varepsilon_0 \\ \varepsilon_1 \end{Bmatrix} = A_{mat} \cdot \varepsilon_b \quad (5)$$

Laminate constitutive equation for transverse shear in terms of shear force resultant can be stated as

$$Q = A_s \cdot \varepsilon_s \quad (6)$$

A , B , D , and A_s are laminate stiffness coefficients representing in-plane, bending-stretching coupling, bending and transverse shear stiffnesses respectively. They are obtained as:

$$\{A, B, D\} = \sum_{k=1}^n \int_A E_x^{(k)} \cdot \{1, z, z^2\} dA_c^{(k)} \quad (7)$$

$$A_s = \sum_{k=1}^n k_s \cdot \int_A \bar{Q}_{55}^{(k)} dA_c^{(k)}$$

where $k_s = 1/2$ is the shear correction factor for hollow circular cross-sections [13]. $E_x^{(k)}$ is the equivalent elastic modulus for composite layer and it is given as [14]

$$\frac{1}{E_x^{(k)}} = \frac{\cos^4(\theta_k)}{E_{11}} + \left(\frac{1}{G_{12}} - \frac{2\nu_{12}}{E_{11}} \right) \cdot \cos^2(\theta_k) \cdot \sin^2(\theta_k) + \frac{\sin^4(\theta_k)}{E_{22}} \quad (8)$$

$\bar{Q}_{55}^{(k)}$ is the shear modulus of composite layer calculation of which can be found in composite mechanics books.

Static equilibrium equations of a beam can be derived through the virtual work principle. In this context, virtual work principle can be stated as the virtual work of internal forces is equal to the virtual work of external forces.

For a beam in the absence of damping it can be written as

$$\int_0^L \int_A \left(\sigma_x^{(k)} \delta \varepsilon_x + k_s \tau_{zx}^{(k)} \delta \gamma_{zx} \right) dA_c^{(k)} dx = \int_0^L q \delta w_0 dx + \sum_{i=1} F_i \delta w_i \quad (9)$$

where $q(x)$ is the distributed load on the beam and F_i is the concentrated load on the corresponding node. In (9), the terms on the left-hand side denote the virtual work of internal forces due to stresses. First term on the right hand side denotes the virtual work of external forces due to distributed load and second term indicates the virtual work of concentrated forces.

Equation (9) can be written in terms of force and moment resultants as

$$\int_0^L [N_1 \delta \varepsilon_0 + N_2 \delta \varepsilon_1 + Q \delta \varepsilon_s] dx = \int_0^L q \delta w_0 dx + \sum_{i=1} F_i \delta w_i \quad (10)$$

Using virtual work equation (10), equation of motion can be obtained in matrix form as:

$$\mathbf{P} = \mathbf{F} \quad (11)$$

where \mathbf{P} and \mathbf{F} denote internal force and external force vectors, respectively. Nonlinear static equation of equilibrium in (11) can be solved by using iterative Newton Raphson method. In the implicit solution procedure, equation of equilibrium is written in residual form where displacements are to be calculated as:

$$\mathbf{R} = \mathbf{P} - \mathbf{F} \quad (12)$$

Residual equation is linearized leading to the incremental equilibrium equation as

$$\mathbf{K} \Delta \mathbf{U} = -\mathbf{R} \quad (13)$$

Solution of (13) iteratively leads to displacement increments. Displacement increments are added to the previous values to yield final displacement values.

\mathbf{K} matrix in (13) is often referred to as tangent stiffness matrix and for thick straight beam it is given as

$$\mathbf{K} = \int_0^L [N_d^T N_p N_d + N_d^T B_b^T A_{mat} B_b N_d + N_d^T B_s^T A_s B_s N_d] dx \quad (14)$$

where B_b , B_s , N_p , N_d are given as

$$B_b = \begin{bmatrix} 0 & 0 & 0 & 1 & \frac{\partial w_0}{\partial x} & 0 \\ 0 & 0 & 0 & 0 & 0 & 1 \end{bmatrix} \quad (15)$$

$$B_s = [0 \quad 0 \quad 1 \quad 0 \quad 1 \quad 0] \quad (16)$$

$$N_p = \begin{bmatrix} 0 & 0 & 0 & 0 & 0 & 0 \\ 0 & 0 & 0 & 0 & 0 & 0 \\ 0 & 0 & 0 & 0 & 0 & 0 \\ 0 & 0 & 0 & 0 & 0 & 0 \\ 0 & 0 & 0 & 0 & N_1 & 0 \\ 0 & 0 & 0 & 0 & 0 & 0 \end{bmatrix} \quad (17)$$

Tangent stiffness matrix is calculated using numerical integration. N_d matrix in the tangent stiffness matrix for the i -th integration point (N_d^i) is given as

$$N_d^i = \begin{matrix} \text{Columns:} & 1 & 2 & 3 & \dots & 3i-2 & 3i-1 & 3i & \dots & 3n-2 & 3n-1 & 3n \\ \begin{bmatrix} 0 & 0 & 0 & \dots & 1 & 0 & 0 & \dots & 0 & 0 & 0 \\ 0 & 0 & 0 & \dots & 0 & 1 & 0 & \dots & 0 & 0 & 0 \\ 0 & 0 & 0 & \dots & 0 & 0 & 1 & \dots & 0 & 0 & 0 \\ C_{i1} & C_{i2} & C_{i3} & \dots & C_{i(3i-2)} & C_{i(3i-1)} & C_{i(3i)} & \dots & C_{i(3n-2)} & C_{i(3n-1)} & C_{i(3n)} \\ C_{i1} & C_{i2} & C_{i3} & \dots & C_{i(3i-2)} & C_{i(3i-1)} & C_{i(3i)} & \dots & C_{i(3n-2)} & C_{i(3n-1)} & C_{i(3n)} \\ C_{i1} & C_{i2} & C_{i3} & \dots & C_{i(3i-2)} & C_{i(3i-1)} & C_{i(3i)} & \dots & C_{i(3n-2)} & C_{i(3n-1)} & C_{i(3n)} \end{bmatrix} \end{matrix} \quad (18)$$

where C_{ij} are weighting coefficients used in GDQ method.

III. NUMERICAL RESULTS

GDQ method is used in the solution of super-elliptic composite beam equilibrium equations in this study. In order to employ the GDQ method, a computer program was developed. GDQ code was validated with analysis results from the literature.

For validation, a circular hollow isotropic beam made of stainless steel (SUS304) from the literature is considered [15]. Material properties are: $E=201.04$ GPa, $G=75.8$ GPa and $\nu=0.3262$. Dimensional properties are: $t=0.005$ m, $a=b=0.01$ m, $h=0.02$ m, $L=1$ m. Both ends of the beam are clamped. Comparisons of load-displacement curves under uniformly distributed load with literature and GDQ method are shown in Fig. 3. Good agreement is obtained with the results of the given reference.

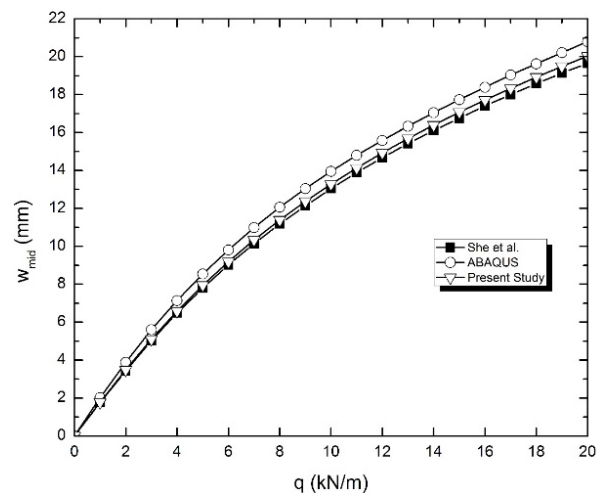


Fig. 3 Comparisons of load-displacement curves for SUS304 beam subjected to uniformly distributed load (q). ($a/b=1$, $a/t=2$, $L/h=50$)

In this study, several super-elliptic composite beam problems are solved with the GDQ method. In the solved examples, different ovality and ellipticity values, layer orientations and boundary conditions are used.

Composite material properties used are: $E_{11}=525.38$ GPa, $E_{22}=E_{33}=21.015$ GPa, $G_{12}=G_{13}=G_{23}=10.508$ GPa, $\rho=775.523$ kg/m³ and $\nu_{12}=0.25$. Two different composite layer angle orientations are used in the analyses: $[0^\circ/90^\circ/0^\circ/90^\circ/0^\circ]$ and $[0^\circ_5]$. Wall thickness of the hollow cross-section (t) is taken as $t=0.0025$ m. Major radius (a) is taken as $a=0.025$ m. The length of the beam is $L=1$ m. $a/t=10$ and $h/b=2$ are utilized in analyses. In all cases, concentrated transverse force is applied ($F=1$ kN) on the free end of the beam for cantilever beam (CF)

and in the middle of the beam for both clamped (CC) and both simply supported (SS) boundary conditions as shown in Fig. 4. Analysis results are obtained using 11 grids with GDQ method.

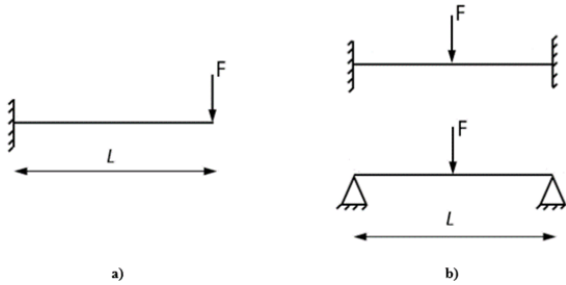


Fig. 4 Loading conditions for (a) cantilever beam (b) beam with CC and SS boundary condition

Transverse displacement values of laminated composite super-elliptic beam with different ovality values for $[0^\circ/90^\circ/0^\circ/90^\circ/0^\circ]$ composite layer orientation under CF, CC and SS boundary condition are given in Figs. 5-7, respectively ($a/b=2$). Transverse displacement values of laminated composite super-elliptic beam with different ovality values for $[0^\circ_5]$ composite layer orientation under CF, CC and SS boundary condition are given in Figs. 8-10, respectively ($a/b=2$). As seen in Figs. 5-10, transverse displacement values decrease with increasing ovality values under CF, CC and SS boundary conditions for $[0^\circ/90^\circ/0^\circ/90^\circ/0^\circ]$ and $[0^\circ_5]$ composite layer orientations. CF boundary condition has led higher displacement values than those for CC and SS boundary conditions. Bending stiffness of $[0^\circ_5]$ composite layer orientation is higher than $[0^\circ/90^\circ/0^\circ/90^\circ/0^\circ]$ layer orientation under CF, CC and SS boundary conditions.

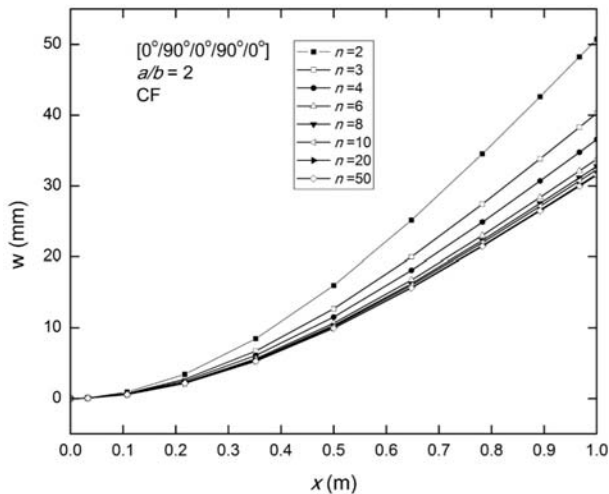


Fig. 5 Transverse displacement values of super-elliptic beam with different ovality values for CF boundary condition ($a/b=2$, $[0^\circ/90^\circ/0^\circ/90^\circ/0^\circ]$)

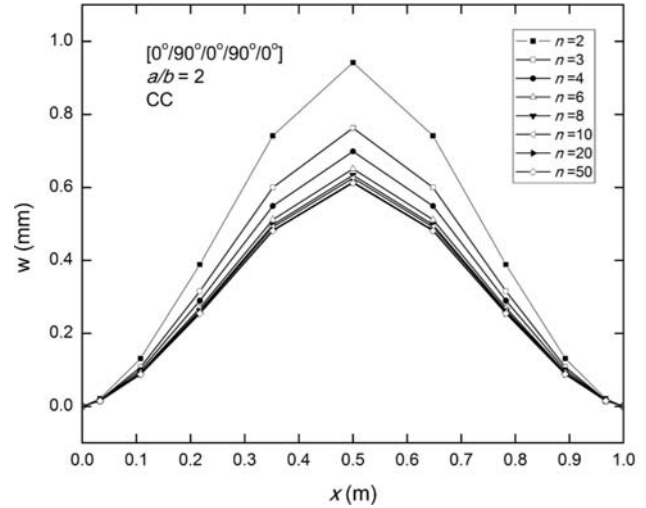


Fig. 6 Transverse displacement values of super-elliptic beam with different ovality values for CC boundary condition ($a/b=2$, $[0^\circ/90^\circ/0^\circ/90^\circ/0^\circ]$)

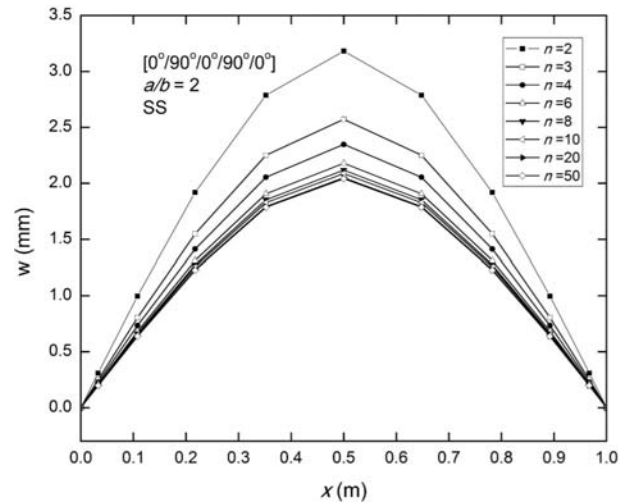


Fig. 7 Transverse displacement values of super-elliptic beam with different ovality values for SS boundary condition ($a/b=2$, $[0^\circ/90^\circ/0^\circ/90^\circ/0^\circ]$)

Maximum transverse displacement values of laminated composite super-elliptic beam with different ellipticity (a/b) and ovality values under CF, CC and SS boundary condition for $[0^\circ/90^\circ/0^\circ/90^\circ/0^\circ]$ layer orientation are shown in Figs. 11-13. As seen in Figs. 11-13, maximum transverse displacement values increase with increasing ellipticity values. However, increase in ovality decreases the displacement values for all ellipticity values ($0.5 \leq a/b \leq 2.5$) and boundary conditions (CF, CC and SS).

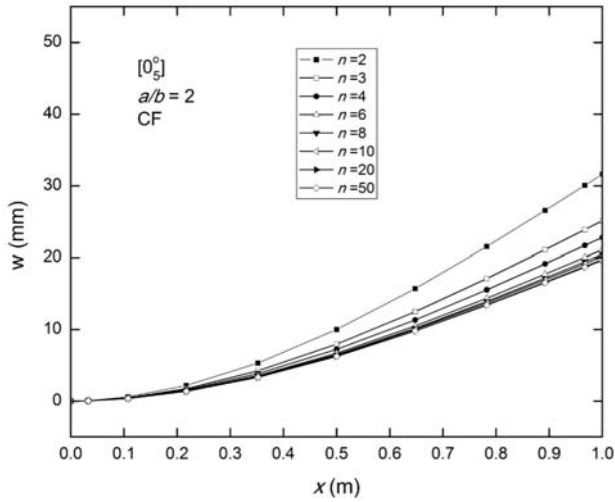


Fig. 8 Transverse displacement values of super-elliptic beam with different ovality values for CF boundary condition ($a/b=2$, $[0_s^0]$)

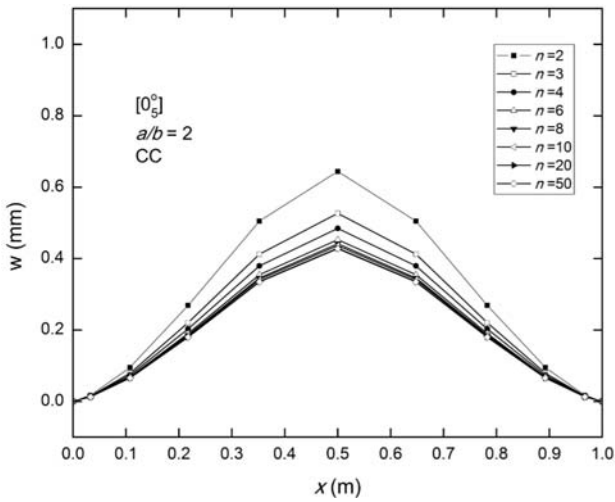


Fig. 9 Transverse displacement values of super-elliptic beam with different ovality values for CC boundary condition ($a/b=2$, $[0_s^0]$)

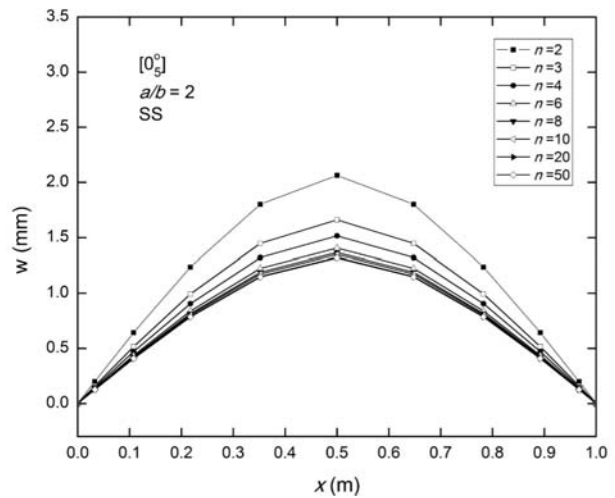


Fig. 10 Transverse displacement values of super-elliptic beam with different ovality values for SS boundary condition ($a/b=2$, $[0_s^0]$)

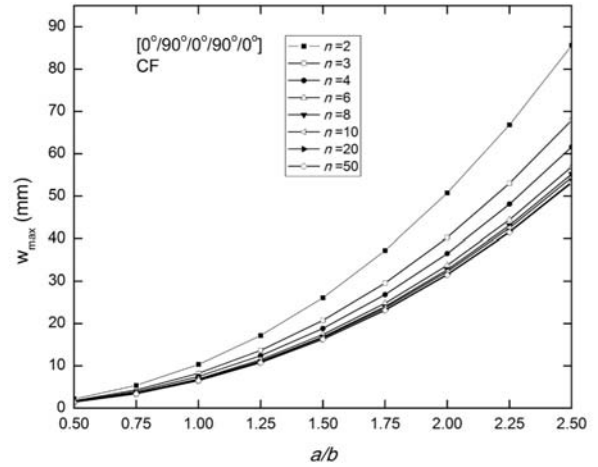


Fig. 11 Maximum transverse displacement values of super-elliptic beam with different ellipticity (a/b) and ovality values for CF boundary condition (For $[0^0/90^0/0^0/90^0/0^0]$ layer orientation)

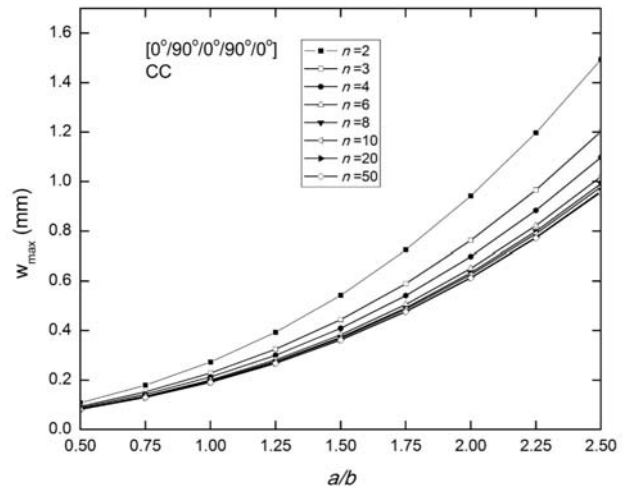


Fig. 12 Maximum transverse displacement values of super-elliptic beam with different ellipticity (a/b) and ovality values for CC boundary condition (For $[0^0/90^0/0^0/90^0/0^0]$ layer orientation)

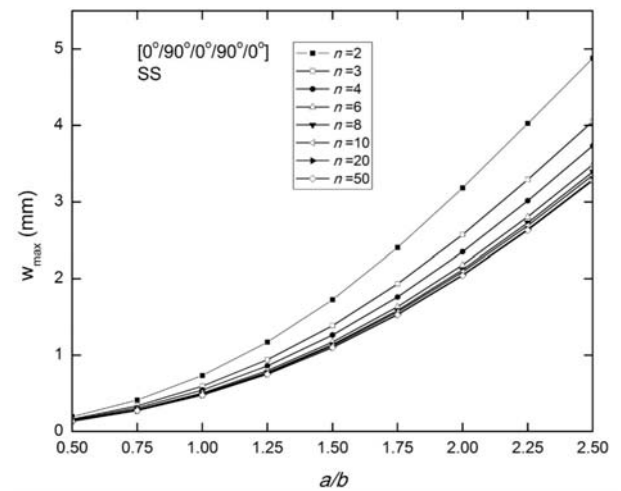


Fig. 13 Maximum transverse displacement values of super-elliptic beam with different ellipticity (a/b) and ovality values for SS boundary condition (For $[0^0/90^0/0^0/90^0/0^0]$ layer orientation)

IV. CONCLUSIONS

In this study, geometrically nonlinear static behavior of laminated composite hollow super-elliptic beams is investigated using GDQ method. Super-ellipse formulation is used to represent the oval, elliptic and circular cross-sections. Virtual work principle is used to obtain equilibrium equations of super-elliptic beam and von-Kármán nonlinear strain-displacement relations are utilized. FSDT is considered to represent transverse shear effect. GDQ method is used to calculate the spatial derivatives in strains and Newton-Raphson method is utilized to solve static equilibrium equations.

Regarding the examples solved in this study, outlines of the study can be summarized as below:

- Transverse displacement values decrease with increasing ovality values under CF, CC and SS boundary conditions for $[0^\circ/90^\circ/0^\circ/90^\circ/0^\circ]$ and $[0^\circ_s]$ composite layer orientations.
- Bending stiffness of $[0^\circ_s]$ composite layer orientation is higher than $[0^\circ/90^\circ/0^\circ/90^\circ/0^\circ]$ layer orientation under CF, CC and SS boundary conditions.
- CF boundary condition has led higher displacement values than those for CC and SS boundary conditions.
- Maximum transverse displacement values increase with increasing ellipticity values for CF, CC and SS boundary conditions.
- GDQ method is an efficient and effective method to analyze such systems like in this study.

REFERENCES

- [1] L. Guo, S. Yang, H. Jiao, "Behavior of thin-walled circular hollow section tubes subjected to bending," *Thin-Walled Structures*, vol. 73, pp. 281-289, 2013.
- [2] D. Karagiozova, T. X. Yu, G. Lu, X. Xiang, "Response of a circular metallic hollow beam to an impulsive loading," *Thin-Walled Structures*, vol. 80, pp. 80-90, 2014.
- [3] D. Karagiozova, T. X. Yu, G. Lu, "Transverse blast loading of hollow beams with square cross-sections," *Thin-Walled Structures*, vol. 62, pp. 169-178, 2013.
- [4] B. Zheng, G. Shu, L. Xin, R. Yang, Q. Jiang, "Study on the Bending Capacity of Cold-formed Stainless Steel Hollow Sections," *Structures*, vol. 8, pp. 63-74, 2016.
- [5] Z. Li, D. Yang, "Thermal post buckling analysis of anisotropic laminated beams with tubular cross-section based on higher-order theory," *Ocean Engineering*, vol. 115, pp. 93-106, 2016.
- [6] H. Asadi, M. M. Aghdam, "Large amplitude vibration and post-buckling analysis of variable cross-section composite beams on nonlinear elastic foundation," *International Journal of Mechanical Sciences*, vol. 79, pp. 47-55, 2014.
- [7] Y. Zhao, Y. Huang, M. Guo, "A novel approach for free vibration of axially functionally graded beams with non-uniform cross-section based on Chebyshev polynomials theory" *Composite Structures*, vol. 168, pp. 277-284, 2017.
- [8] E. Ghafari, J. Rezaeepazhand, "Isogeometric analysis of composite beams with arbitrary cross-section using dimensional reduction method" *Computer Methods in Applied Mechanics and Engineering*, vol. 318, pp. 594-618, 2017.
- [9] P. Jiao, W. Borchani, H. Hasni, A. Alavi, N. Lajnef, "Post-buckling response of non-uniform cross-section bilaterally constrained beams" *Mechanics Research Communications*, vol. 78, pp. 42-50, 2016.
- [10] K. H. Law, L. Gardner, "Lateral instability of elliptical hollow section beams" *Engineering Structures*, vol. 37, pp. 152-166, 2012.
- [11] J. Murin, V. Goga, M. Aminbaghai, J. Hrabovsky, T. Sedlar, H. A. Mang, "Measurement and modelling of torsional warping free vibrations

of beams with rectangular hollow cross-sections" *Engineering Structures*, vol. 136, pp. 68-76, 2017.

- [12] J. N. Reddy, "Geometrically Nonlinear Transient Analysis of Laminated Composite Plates" *AIAA Journal*, vol. 21(4), pp. 621-628, 1983.
- [13] G. R. Cowper, "The Shear Coefficient in Timoshenko's Beam Theory" *Journal of Applied Mechanics*, vol. 33(2), pp. 335-340, 1966.
- [14] M. Hajianmaleki, M. S. Qatu, "Static and vibration analyses of thick, generally laminated deep curved beams with different boundary conditions" *Composite Part B: Eng*, vol. 43, pp. 1767-75, 2012.
- [15] G. She, F. Yuan, Y. Ren, "Nonlinear analysis of bending, thermal buckling and post-buckling for functionally graded tubes by using a refined beam theory" *Composite Structures*, vol. 165, pp. 74-82, 2017.